Drug Design, Development and Therapy

Dovepress
open access to scientific and medical research

Open Access Full Text Article

ORIGINAL RESEARCH

Integrating Network Pharmacology and Bioinformatics to Explore the Effects of Dangshen (*Codonopsis pilosula*) Against Hepatocellular Carcinoma: Validation Based on the Active Compound Luteolin

Yaping Yu[1,*], Shun Ding[2,*], Xiaoqing Xu[1,*], Dongming Yan[3], Yonghao Fan[1], Banzhan Ruan[1], Xiaodian Zhang[1], Liping Zheng[1], Wei Jie[1], Shaojiang Zheng[1,4]

[1]Department of Oncology of the First Affiliated Hospital & Tumor Institute, Hainan Medical University, Haikou, 570102, People's Republic of China; [2]Department of Otolaryngology, Head and Neck Surgery, the First Affiliated Hospital, Hainan Medical University, Haikou, 570102, People's Republic of China; [3]Department of Neurosurgery, the First Affiliated Hospital of Hainan Medical University, Haikou, 570102, People's Republic of China; [4]Key Laboratory of Emergency and Trauma, Ministry of Education, Hainan Medical University, Haikou, 571199, People's Republic of China

*These authors contributed equally to this work

Correspondence: Wei Jie; Shaojiang Zheng, Department of Oncology of the First Affiliated Hospital & Tumor Institute, Hainan Medical University, Haikou, 570102, People's Republic of China, Tel +86-898-66968217; +86-898-66568158, Email wei_jie@hainmc.edu.cn; zhengsj2008@163.com

Purpose: This study aimed to explore the pharmacological mechanism of Dangshen (*Codonopsis pilosula*) against hepatocellular carcinoma (HCC) based on network pharmacology and bioinformatics, and to verify the anticancer effect of luteolin, the active ingredient of *Codonopsis pilosula*, on HCC cells.

Methods: The effective compounds and potential targets of *Codonopsis pilosula* were established using the Traditional Chinese Medicine Systems Pharmacology Database and Analysis Platform (TCMSP) database. The genes related to HCC were obtained through the GeneCards database. The interactive genes were imported into the Visualization and Integrated Discovery database for Gene Ontology (GO) annotation and Kyoto Encyclopedia of Genes and Genomes (KEGG) signal enrichment, and the hub genes were screened out. The Cancer Genome Atlas database was used to construct a prognosis model, and the prognosis and clinicopathological correlation were analyzed. In in vitro experiments, we verified the effects of luteolin, an active compound of *Codonopsis pilosula*, on the proliferation, cell cycle, apoptosis and migration of HCC cells.

Results: A total of 21 effective compounds of *Codonopsis pilosula* and 98 potential downstream target genes were screened through the TCMSP database, and 1406 HCC target genes were obtained through the GeneCards database. Finally, 53 interacting genes between the two databases were obtained, among which, the 10 key node genes were *CASP3, TP53, MDM2, AKT1, ESR1, BCL2L1, MCL1, HSP90AA1, CASP9*, and *CCND1*, involving 77 typical GO terms and 72 KEGG signals. The Kaplan–Meier survival curve of the model group showed that the overall survival of the low-risk group was significantly higher than that of the high-risk group. Luteolin significantly inhibited the proliferation and migration of HCC cells, induced apoptosis, and increased the G2/M phase ratio. Mechanistically, luteolin significantly inhibited the phosphorylation of MAPK-JNK and Akt (Thr308) and subsequently led to upregulation of ESR1. Pharmacological inhibition of ESR1 with fulvestrant enhanced cell viability and migration and attenuated apoptosis.

Conclusion: *Codonopsis pilosula* has potential for clinical development due to its anti-HCC properties. Luteolin, the effective component of *Codonopsis pilosula*, plays anti-HCC role through AKT- or MAPK-JNK signaling mediated ESR1.

Keywords: *Codonopsis pilosula*, network pharmacology, bioinformatics, luteolin, hepatocellular carcinoma

Received: 27 August 2022
Accepted: 22 February 2023
Published: 1 March 2023

Introduction

Liver cancer was the sixth most common cancer and the fourth leading cause of cancer worldwide in 2018.[1] In 2020, there were 905,677 new cases and 830,180 deaths from liver cancer worldwide, accounting for the third highest rate of cancer incidence and death.[2] In China, there were an estimated 431,383 new cases and 412,216 deaths for liver cancer in 2022,[3] and the burden of liver cancer remains high.[4] Therefore, strengthening research on liver cancer prevention and treatment is an urgent clinical need.

Hepatocellular carcinoma (HCC) is the most common form of primary liver cancer. Due to advances in the models, molecular classification, and biomarkers for HCC, the number of effective clinical treatments is increasing.[5–7] Traditional Chinese medicine (TCM) has the advantages of wide availability, multi-target, toxicity reduction, and enhanced efficacy. Recently, TCM has also shown advantages in inhibiting tumor growth and preventing recurrence, with good prospects. Moreover, increasing reports have highlighted the efficacy of Chinese medicine as adjuvant therapy for HCC.[8–11] Dangshen (*Codonopsis pilosula*), a perennial herb containing saponins, polysaccharides, and sterols, is known to have anti-inflammatory,[12] anti-oxidative stress,[13,14] and immune modulatory functions,[15,16] while its anti-cancer properties have also been gradually discovered. *Codonopsis pilosula* is thought to have therapeutic effects on tumors such as gastric cancer,[17] melanoma,[18,19] and osteosarcoma,[20] which has increased research interest surrounding the use of *Codonopsis pilosula* in HCC.

Recently, network pharmacology has received increased attention as a means to predict the pharmacological mechanisms of drugs for treating HCC.[21–23] In this study, we applied network pharmacology technology to screen for overlapping genes for geometric and Kyoto Encyclopedia of Genes and Genomes (KEGG) analyses of the pathogenicity of *Codonopsis pilosula* targeting HCC. Additionally, we constructed a prognostic model for the prognosis and clinico-pathological staging of HCC, and finally validated the anti-HCC effect of luteolin, an active compound of *Codonopsis pilosula*, through in vitro cytological experiments.

Materials and Methods

Excavation and Screening of Effective Compounds and Their Targets in *Codonopsis pilosula*

The Traditional Chinese Medicine Systems Pharmacology Database and Analysis Platform (TCMSP) is a database that was established based on the framework of TCM system pharmacology and provides 12 important pharmacokinetic properties, such as oral bioavailability (OB) and drug-likeness (DL), which are mainly used to screen and evaluate pharmaceutical compounds.[24] The TCMSP was used to screen *Codonopsis pilosula* for active compounds (set OB ≥ 30% and DL ≥ 0.18) and to predict the target genes corresponding to the active compounds. All of the gene names were converted into "GENE SYMBOL" format by the STRING database (https://string-db.org/) to search for protein interactions.

Screening for HCC-Related Disease Genes

The GeneCards database (https://www.genecards.org/) was used to screen HCC-related genes, and SCORE > 0.5 was set as the criteria to screen out the target genes for HCC.

Construction of a "Compound-Interacting Gene" Network for *Codonopsis pilosula*

The effective compound target genes and disease target genes of *Codonopsis pilosula* were produced by Venny 2.1.0 (https://bioinfogp.cnb.csic.es/tools/venny/index.html), and the interacting genes were established by the Venny diagram. The network analysis map of compound-interacting genes was constructed by Cytoscape 3.6.0 (http://manual.cytoscape.org/en/3.6.0/).

Constructing the Protein Interaction Network

The interacting genes were entered into the "Multiple proteins" module of the STRING database with a confidence score >0.4, and the protein-to-protein interaction (PPI) network of the target genes was retrieved and analyzed using Cytoscape

software with the cytoHubba module. The protein interaction network of key node genes was constructed, and the top 10 genes in the network were selected as the key node genes for *Codonopsis pilosula* anti-cancer treatment according to the Degree value.

Gene Ontology and Kyoto Encyclopedia of Genes and Genomes Pathway Enrichment Analyses

The Database for Annotation, Visualization and Integrated Discovery (DAVID, https://david.ncifcrf.gov/) is a bioinformatics database for screening gene and protein collections for biologically relevant data,[18] and enrichment analysis of target genes in the "compound-interacting gene" network, including Gene Ontology (GO) and KEGG enrichment analysis. The GO and KEGG pathway enrichment analyses were ranked according to *P* values.

Prognostic Model Construction

Based on the top 10 key node genes, corresponding sequencing clinical information for HCC was obtained from The Cancer Genome Atlas (TCGA) dataset (https://portal.gdc.com). Log rank was used to conduct Kaplan–Meier survival analysis by median risk score to divide the samples into high- and low-risk groups, and the survival differences between the two groups were compared. Subsequently, timeROC analysis was performed to compare the predictive accuracy and risk scores of key node genes. The least absolute shrinkage and selection operator (LASSO) regression algorithm was used for feature selection to screen prognosis-related genes, and 10-fold cross-validation was used for the above analysis using the R package "glmnet." Survival analysis of prognosis genes was performed by Gene Expression Profiling and Interactive Analysis (GEPIA, http://gepia2.cancer-pku.cn/#index) to initially screen for potential HCC prognostic markers and to analyze the relationship between the gene expression level and the clinicopathological staging of HCC.

Cell Culture and Drug Treatment

HepG2 cells (Cell Bank of Chinese Academy of Sciences) were suspended in DMEM (BI, Israel) containing 10% fetal bovine serum (FBS; Gibco) and incubated at 37°C with 5% CO_2. To evaluate the effect of luteolin on HepG2 cells, 5, 10, 20, 40, 80, 160, and 320 μmol/L luteolin (Sigma) was used. To determine the effect of ESR1 inhibition on HepG2 cells, 1, 20, 50, 100, 300, 500, and 900 nmol/L fulvestrant (Selleck China) was used. To determine the effect of Akt and MAPK-JNK signaling on ESR1 expression, Akt agonist SC79 (10 μmol/L, Selleck China), and MAPK-JNK agonist anisomycin (4 μmol/L, Selleck China) were used. DMSO served as a control.

CCK-8 Assay

A total of 5000 HepG2 cells in a total volume of 100 μL complete DMEM were added to each well of 96-well plates. After one night of recovery, various concentrations of luteolin and fulvestrant were added, and DMSO served as a control. Following a 48-h incubation, the CCK-8 reagents (Beyotime Biotechnology) were added and incubated for an additional 2 h. Finally, the absorbance (OD) was measured at 450 nm using a plate reader (BIOTEK), and the half inhibition rate (IC50) was calculated. The individual groups were repeated across six wells, and experiments were performed in triplicate.

Wound-Scratch Assay

HepG2 cells were added to six-well plates until a monolayer fusion state was reached, following which, the cells were synchronized overnight with DMEM + 0.5% FBS. Three parallel scratches per well were made with 200-μL pipette tips, and the wells were rinsed with phosphate-buffered saline (PBS) buffer to remove the unattached cells. The cells were subsequently incubated in DMEM supplemented with 2% FBS and 50 μmol/L luteolin, with DMSO (0.1%) used as the control group, and incubated at 37°C in a 5% CO_2 incubator for 24 h. Following incubation, the wounds were photographed at 0 and 24 h post scratching, and the values for the closed wound (%) were calculated using ImageJ software (https://imagej.net/downloads). Experiments were performed in triplicate.

Flow Cytometry Analysis of Cell Cycle and Apoptosis

HepG2 cells were added to 6-cm dishes and incubated with DMEM containing 50 μmol/L luteolin and 300 nmol/L fulvestrant at 37°C, and 5% CO_2 for 48 h. Following incubation, the cells were collected and subjected to cell cycle and apoptosis analysis. A PI/RNase Staining Buffer Cell Cycle Assay Kit (BD Pharmingen) was used for cell cycle analysis, and an FITC-coupled Annexin-V Apoptosis Assay Kit (BD Pharmingen) was employed for apoptosis detection. Experiments were performed in triplicate.

Western Blotting

Total protein was extracted using RIPA buffer (Beyotime) and quantitated using a BCA kit (Procell). First, 30 μg total protein was subjected to 10% SDS-PAGE gel electrophoresis and transferred to PVDF membranes. Subsequently, the membranes were incubated with the following primary antibodies overnight at 4°C: ESR1 (Proteintech,1:1000), p-AKT (PTM, 1:800), p-JNK (Proteintech, 1:1000), and β-actin (PTM, 1:1000). After washing with TBST buffer, the membranes were incubated with the appropriate HRP-coupled IgGs for 1.5 h at room temperature, before visualizing by chemiluminescence using ECL (Procell) detection reagents. Finally, the gray scale values were analyzed with ImageJ software. Experiments were performed in triplicate.

Statistical Analysis

The TCMSP, GeneCards, Venny, STRING, DAVID, TCGA, and GEPIA public databases were used to conduct pharmacology and bioinformatics analyses. The relevant data and statistics were evaluated using the corresponding algorithm of the databases or R software. For in vitro experiments, SPSS software (version 26.0, IBM Corporation, Armonk, NY, USA) was used for statistical analysis, and images were plotted using GraphPad Prism (version 9.0, GraphPad Software Inc., La Jolla, CA, USA). Shapiro–Wilk test and Q-Q plot were used to assess data distributions, the measurement data conforming to normal distribution were expressed by mean ± standard deviation (SD), and analyzed by *t*-test. While non-normally distributed measurement data were expressed as median (interquartile range), and the comparisons were examined by Mann–Whitney test. Dunnett test in one-way analysis of variance (ANOVA) was used for comparison between multiple groups. P values <0.05 were considered statistically significant.

Results

Basic Information on the Effective Compounds of *Codonopsis pilosula*

The TCMSP database was used to mine and screen the effective compounds of *Codonopsis pilosula*, and 21 effective compounds were screened according to the set OB and DL values as criteria (Table 1).

Analysis of the Active Compounds of *Codonopsis pilosula* and HCC Target Genes

The TCMSP database was used to predict the target genes of 21 effective compounds of *Codonopsis pilosula*, and the STRING database was used to convert all target gene names into "GENE SYMBOL" format. A total of 98 genes were obtained. The GeneCards database was used to screen the target genes of HCC-related diseases, and 1406 target genes of HCC were screened by setting SCOR > 0.5 as the parameter criteria, suggesting the complexity of HCC carcinogenesis. Venny was used to analyze the 98 target genes of the effective compounds of *Codonopsis pilosula* and of the 1406 HCC-related disease target genes, 53 of the interaction genes were enriched (Figure 1A).

Compound-Interacting Gene Network Map

Network analysis of the "compound-interacting gene" was constructed by Cytoscape, and the effective compounds with the most interacting genes in the network were luteolin, spinasterol, and glycitein (Figure 1B). The active compounds with interaction genes may be an important material basis for the anticancer effect of *Codonopsis pilosula*.

Table 1 Information on the 21 Effective Compounds of *Codonopsis pilosula*

Molecule ID	Molecule Name	OB (%)	DL
MOL002879	Diop	43.59	0.39
MOL003896	7-Methoxy-2-methyl isoflavone	42.56	0.20
MOL008407	(8S,9S,10R,13R,14S,17R)-17-[(E,2R,5S)-5-ethyl-6-methylhept-3-en-2-yl]-10,13-dimethyl-1,2,4,7,8,9,11,12,14,15,16,17-dodecahydrocyclopenta[a]phenanthren-3-one	45.40	0.76
MOL005321	Frutinone A	65.90	0.34
MOL008397	Daturilin	50.37	0.77
MOL008391	5alpha-Stigmastan-3,6-dione	33.12	0.70
MOL007514	Methyl icosa-11,14-dienoate	39.67	0.23
MOL006554	Taraxerol	38.40	0.77
MOL000449	Stigmasterol	43.83	0.76
MOL001006	Poriferasta-7,22E-dien-3beta-ol	42.98	0.76
MOL004355	Spinasterol	42.98	0.76
MOL006774	Stigmast-7-enol	37.42	0.75
MOL007059	3-Beta-(hydroxymethyllenetanshiquinone	32.16	0.41
MOL003036	ZINC03978781	43.83	0.76
MOL002140	Perlolyrine	65.95	0.27
MOL008400	Glycitein	50.48	0.24
MOL004492	Chrysanthemaxanthin	38.72	0.58
MOL008411	11-Hydroxyrankinidine	40.00	0.66
MOL008393	7-(beta-xylosyl) cephalomannine_qt	38.33	0.29
MOL000006	Luteolin	36.16	0.25
MOL008406	Spinoside A	39.97	0.40

Abbreviations: OB, oral bioavailability; DL, drug likeness.

PPI Network of *Codonopsis pilosula* and HCC Targets

After entering 53 interacting genes in the "Multiple proteins" module of the STRING database and setting the confidence score to >0.4, the protein interactions of the interacting genes were searched, and then the PPI network was displayed using Cytoscape software (Figure 1C). Ten key node genes were selected, namely *CASP3, TP53, MDM2, AKT1, ESR1, BCL2L1, MCL1, HSP90AA1, CASP9*, and *CCND1*, and the relationships and importance of key node genes in the PPI network were shown by this network (Figure 1D).

GO Terms and KEGG Pathway Enrichment

The 53 interacting genes were entered into the DAVID database for functional annotation. A total of 77 GO terms were obtained, the full details of which are shown in Table S1. The GO term analysis included biological process (BP), Cellular component (CC), and Molecular function (MF),[25] and the top 10 GO terms are plotted in Figure 2A. GO:0045429~positive regulation of nitric oxide biosynthetic process was the most significant GO-BP, GO:0005654~nucleoplasm was the most significant GO-CC, and GO:0019903~protein phosphatase binding was the most significant GO-MF. A total of 72 KEGG signals were obtained, and the top 10 are plotted in Figure 2B. The full lists of KEGG signals are shown in Table S2.

Prognostic Modeling Based on Key Node Genes

Based on the expression of the 10 key node genes, six genes, including *HSP90AA1, MCL1, ESR1, AKT1, TP53*, and *BCL2L1*, which were related to prognosis were further screened from the LASSO algorithm to construct a prognostic prediction model. The cohort was divided into two groups, with the median risk score value as the threshold (Figure 3A). The tuning parameter of OS-related protein (logλ) was selected for tenfold cross-validation of the error curve, and according to the minimum criterion and 1-se criterion, vertical dashed lines were plotted at the optimal values (Figure 3B).

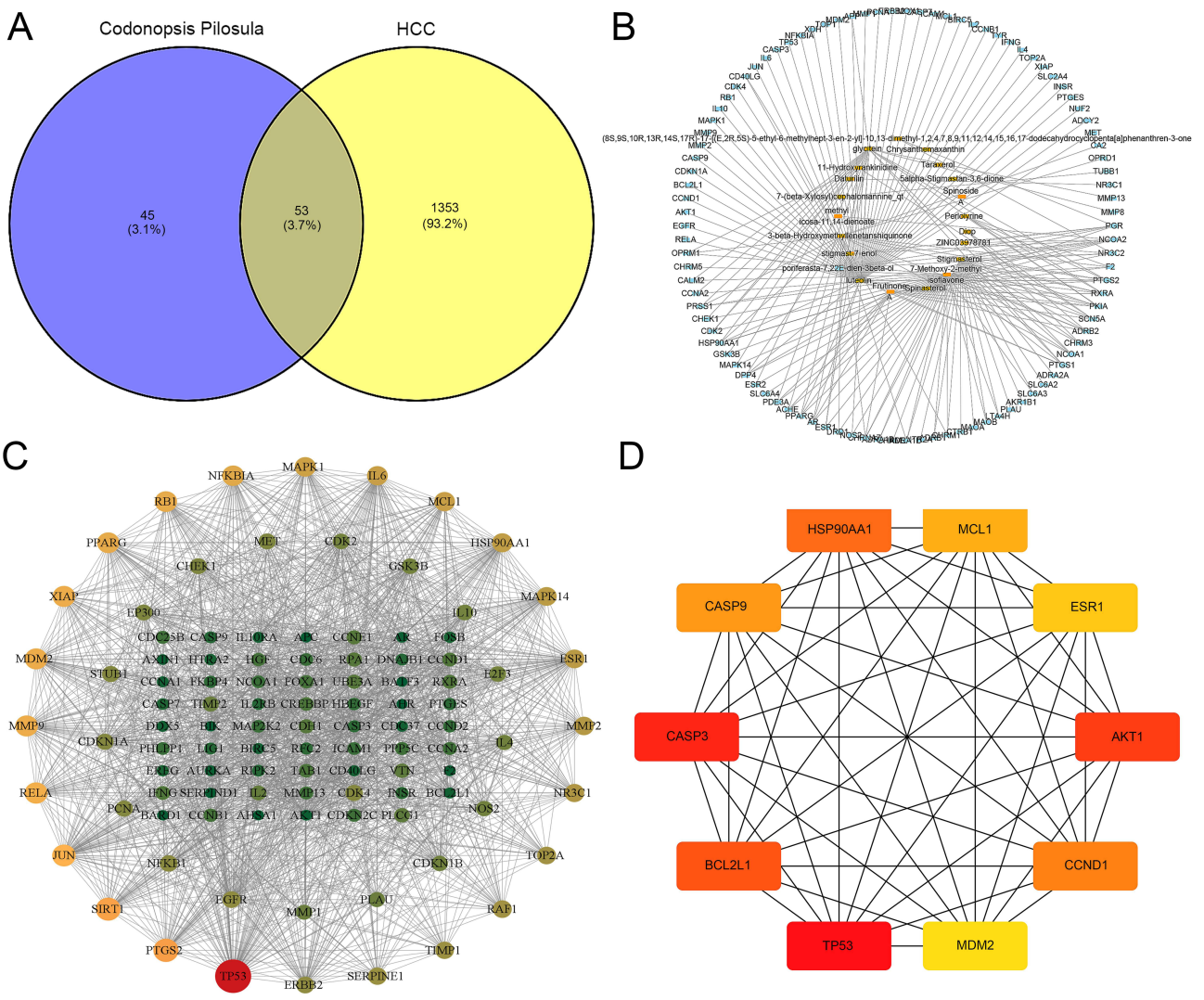

Figure 1 Screening of *Codonopsis pilosula* active compound targets and the interaction network of *Codonopsis pilosula* targets and hepatocellular carcinoma. (**A**) Venny analysis of targets for the effective compounds and hepatocellular carcinoma target genes of *Codonopsis pilosula*. (**B**) Network diagram of *Codonopsis pilosula* compound-interactive genes. Yellow represents Hepatocellular carcinoma-related targets, and green represents the active compound of *Codonopsis pilosula*. (**C**) Network of *Codonopsis pilosula* and hepatocellular carcinoma targets. (**D**) Interaction network of the key hub genes of *Codonopsis pilosula* targets.

TCGA dataset was used to divide the samples into high- and low-risk groups according to gene expression. As the risk score increased, the mortality rate of patients increased at the same time point (Figures 4A and B). Figure 4C shows the heat map of gene expressions in this signature. Further, TCGA dataset was used for Kaplan–Meier curve analysis, and the results indicated that the median survival time was 6.7 years in the low-risk group and 2.5 years in the high-risk group; thus, cohorts with a high-risk score displayed a worse survival (P = 3.46 × 10–8, HR = 2.794, 95% CI = 1.939–4.024, Figure 4D). The time-dependent receiver operating characteristic (ROC) curves were plotted to assess the predictive efficacy, and the results showed 1-, 3-, and 5-year AUCs of 0.722, 0.708, and 0.686, respectively (Figure 4E). The risk score formula was calculated as follows:

Risk score = (0.3068) × *HSP90AA1* + (0.0726) × *MCL1* + (–0.252) × *ESR1* + (0.1638) × *AKT1* + (–0.248) × *TP53* + (0.1231) × *BCL2L1*.

Prognosis, Survival, and Clinicopathological Stages of Patients with HCC

Based on the six prognosis-related genes in the above risk score formula, using the GEPIA database, among these six genes, *ESR1* and *HSP90AA1* were related to the overall survival (OS) of patients with HCC, and only *ESR1* expression

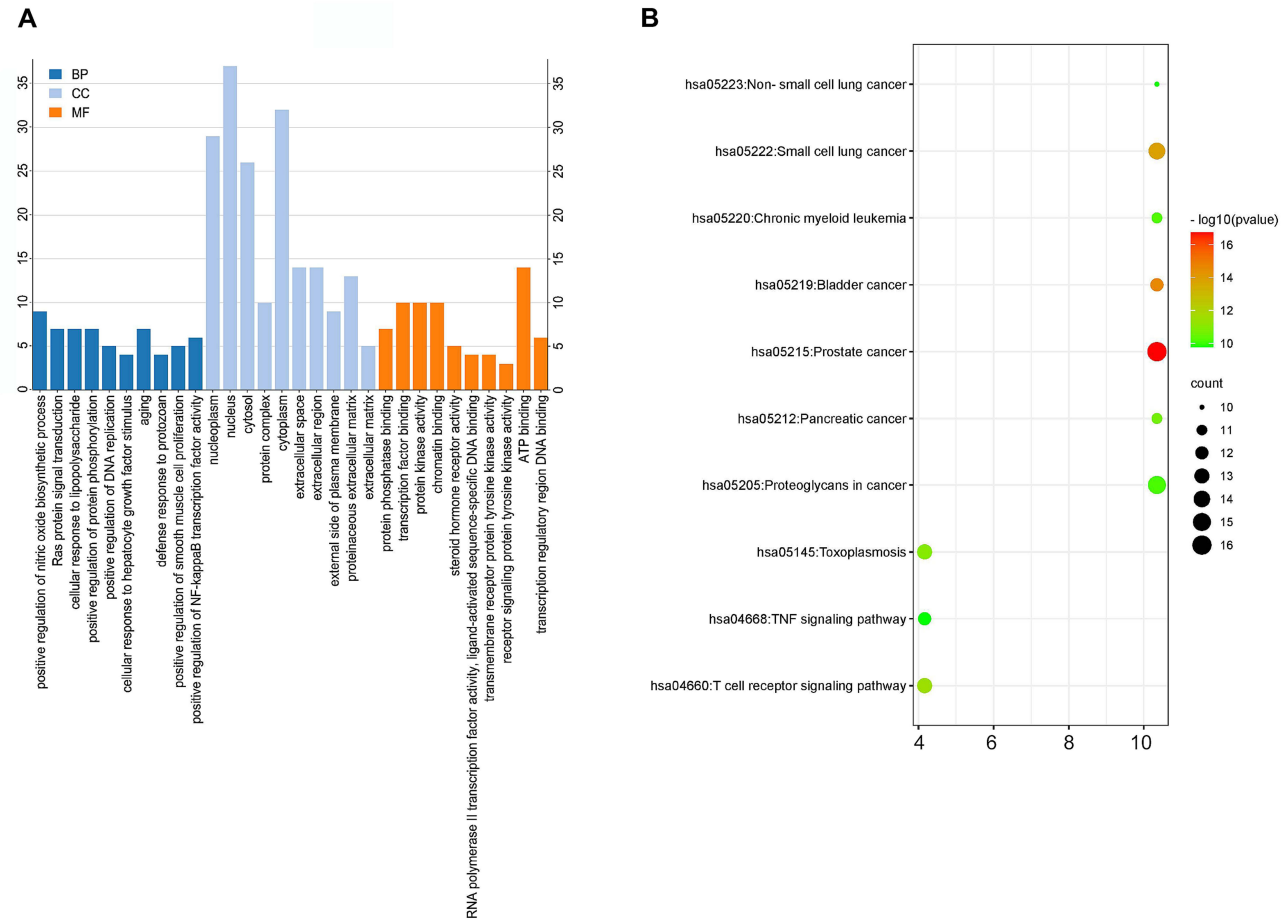

Figure 2 Top 10 GO terms and KEGG signals of overlapping genes between *Codonopsis pilosula* and hepatocellular carcinoma. (**A**) GO terms. (**B**) KEGG pathways. **Abbreviations**: BP. Biological process; CC, cellular component; MF, molecular function.

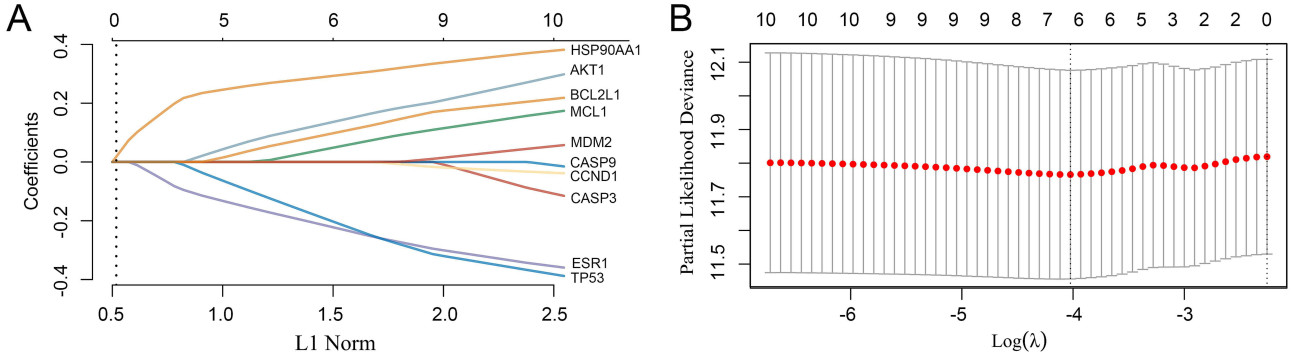

Figure 3 Risk model for patients with hepatocellular carcinoma based on 10 key node genes. (**A**). LASSO coefficient profiles of 10 protein-coding genes. (**B**) LASSO regression with tenfold cross-validation obtained six prognostic genes using the minimum lambda value.

was related to the disease-free survival (DFS) of patients with HCC. The higher the *ESR1* expression, the better the prognosis, and the higher the *HSP90AA1* expression, the worse prognosis of patients with HCC (Figure 5). Furthermore, the above six prognostic genes were analyzed by GEPIA to investigate the relationship between gene expression and the clinicopathological stage of HCC. The results showed that the *ESR1* expression was negatively associated with and clinical stage of HCC, with lower *ESR1* expression associated with worse prognosis of patients with late-stage liver cancer (Figure 6).

https://doi.org/10.2147/DDDT.S386941 DovePress

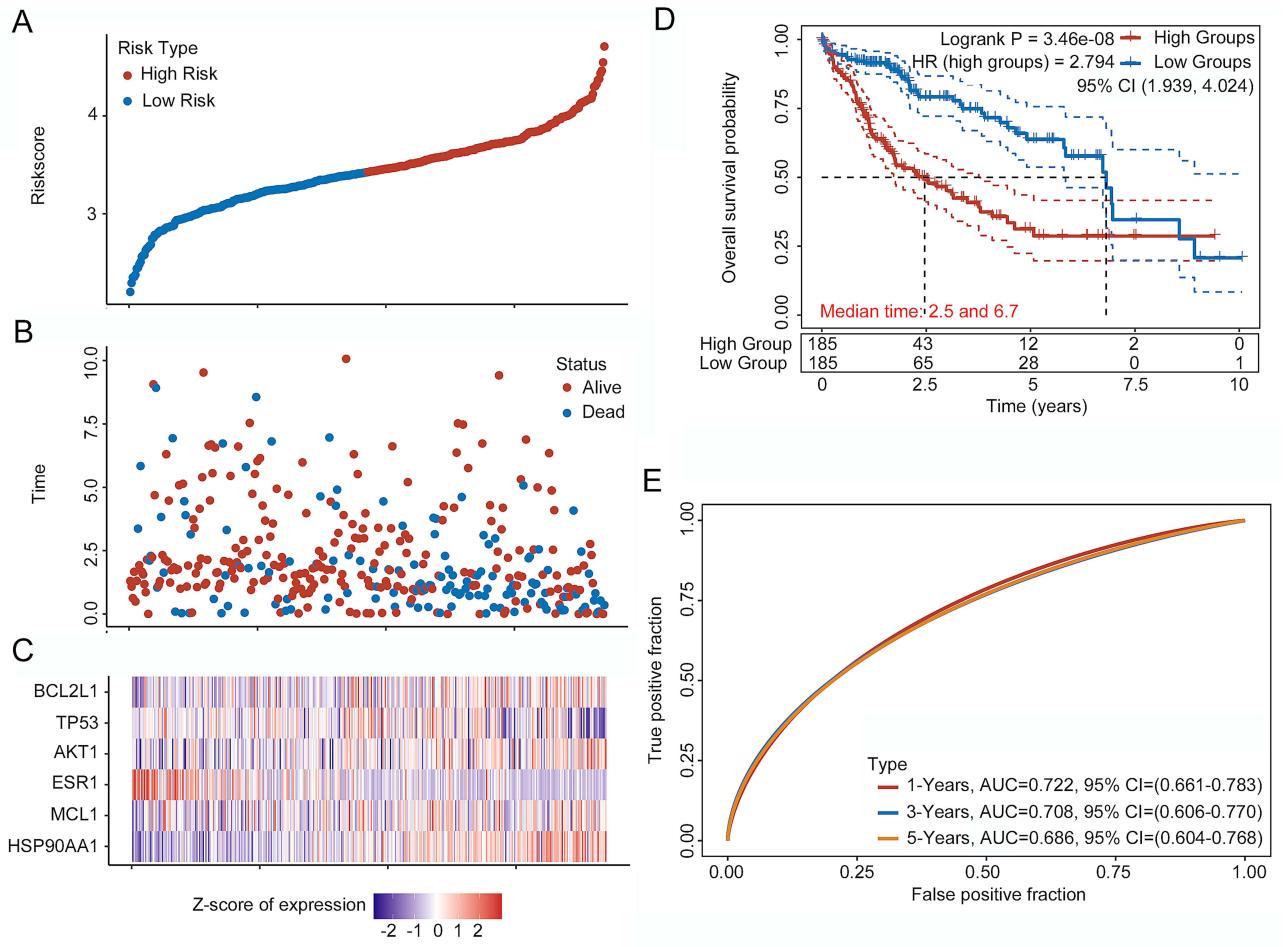

Figure 4 Prognostic analysis of the six-gene signature in the training set. (**A**) Curve of the risk score. (**B**) Survival status of the patients, where increased patient death corresponds to a higher risk score. (**C**) Heatmap of the expression profiles of the six prognostic genes in the low- and high-risk groups. (**D**) Kaplan–Meier survival analysis of the six-gene signature. (**E**) Time-dependent receiver operating characteristic analysis of the six-gene signature.
Abbreviation: AUC, area under the curve.

Impact of Luteolin on HCC Proliferation, Cell Cycle, Migration, and Apoptosis

To validate the impact of *Codonopsis pilosula* on HCC cells, we used luteolin, an active component of *Codonopsis pilosula*, to treat HepG2 cells. As shown in Figure 7A, luteolin inhibited HepG2 viability in a concentration-dependent manner, and the IC50 for HepG2 cells was 70 μmol/L. We then treated HepG2 cells with 50 μmol/L luteolin for the following experiments. As expected, luteolin attenuated HepG2 cell migration (Figure 7B), arrested the cell cycle at the G2/M phase Figures 7C and D), and promoted apoptosis (Figures 7E and F). Finally, considering that AKT and MAPK-JNK signaling are related to cell viability and migration and that these genes were also enriched in several KEGG signals, such as the hsa04660:T cell receptor signaling pathway, the hsa04012:ErbB signaling pathway, and the hsa04630: Jak-STAT signaling pathway, we detected their activation status by Western blotting. As shown in Figures 7G and H, Luteolin indeed inhibited AKT and MAPK-JNK signal activation.

Effects of ESR1 in Luteolin-Anti HCC

Considering that ESR1 has been found to be one of the key node genes involved in the PPI network of *Codonopsis pilosula* and HCC targets and related to the prognosis of HCC, we next determined whether it is involved in the process of luteolin-anti HCC. As we expected, treating HepG2 cells with luteolin led to upregulation of ESR1, while fulvestrant inhibited ESR1 expression (Figures 8A and B). Treating HepG2 cells with Akt agonist SC79 and MAPK-JNK agonist anisomycin resulted in attenuated ESR1 expression (Figures 8C and D). Administration of ESR1 inhibitor fulvestrant in

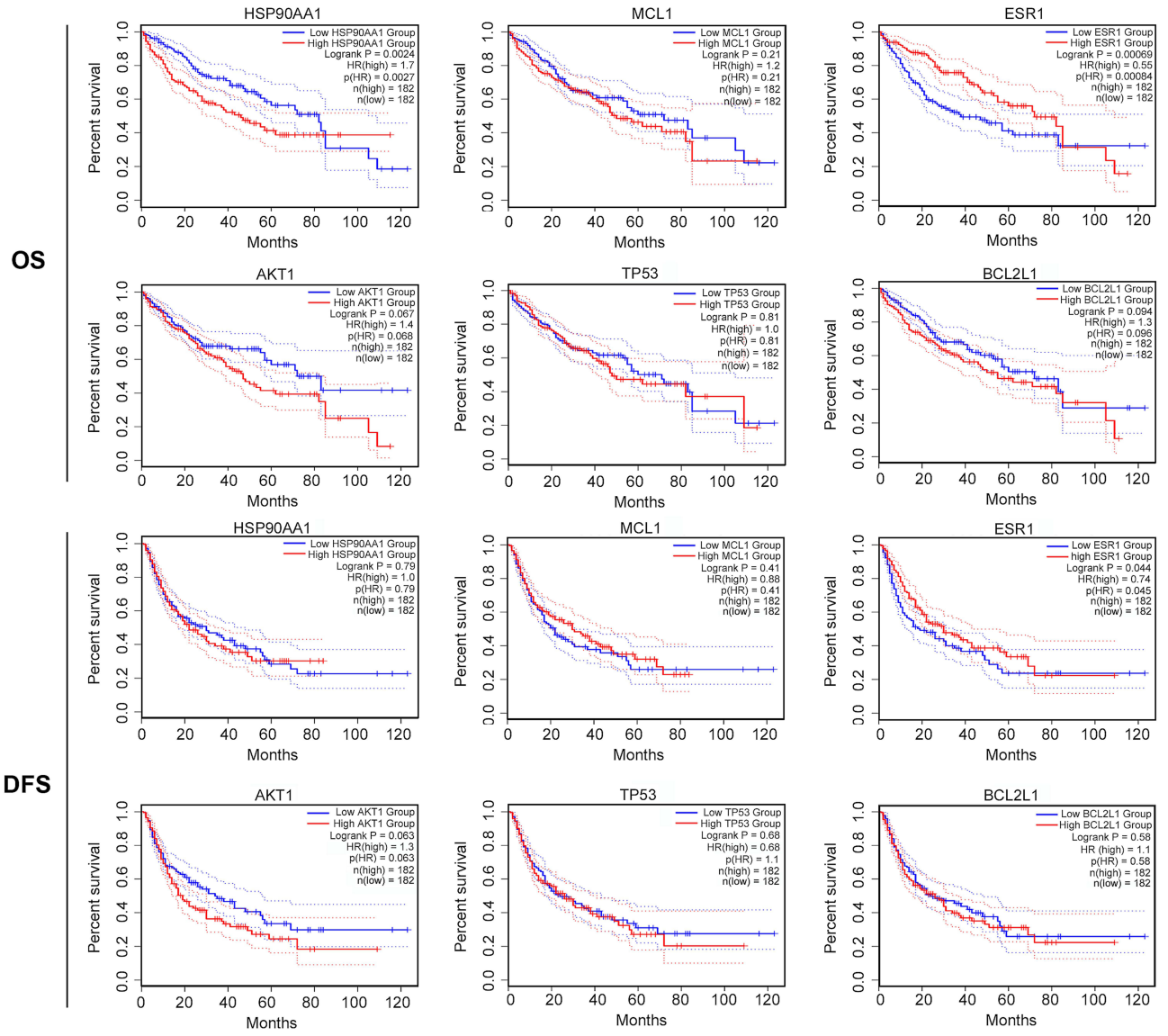

Figure 5 Overall survival (OS) and disease-free survival (DFS) analysis of genes involved in the risk score formula OS and DFS for *HSP90AA1*, *MCL1*, *ESR1*, *AKT1*, *TP53*, and *BCL2L1* in hepatocellular carcinoma plotted according to the Cancer Genome Atlas dataset.
Abbreviations: OS, overall survival; DFS, disease-free survival.

HepG2 cells led to the upregulation of cell viability in a concentration-dependent manner (Figure 8E), followed by the inhibition of apoptosis (Figure 8F) and enhanced cell migration (Figure 8G).

Discussion

In the current study, we adopted network pharmacology technology to explore the effects of *Codonopsis pilosula* on HCC. Firstly, 21 active compounds of *Codonopsis pilosula*, including luteolin, spinasterol, and glycitein, were found through the TCMSP platform. Then, a "compound-interacting gene" network was established, which showed that the active compounds may mediate 98 downstream genes. TCMSP is generally considered to have unique signatures in mining the active ingredients of TCM compounds.[24] The 21 screened active ingredients of *Codonopsis pilosula* provide options for selecting anticancer drugs for the treatment of late-stage disease. Subsequently, potential target genes of HCC and target compounds of *Codonopsis pilosula* were selected. The GeneCards database has recently been adopted to screen the potential targets of various cancers.[26,27] Using this database, we obtained 1404 genes with potential associations with HCC. Finally, 53 genes were obtained by Venny analysis, with hub genes including *CASP3, TP53,*

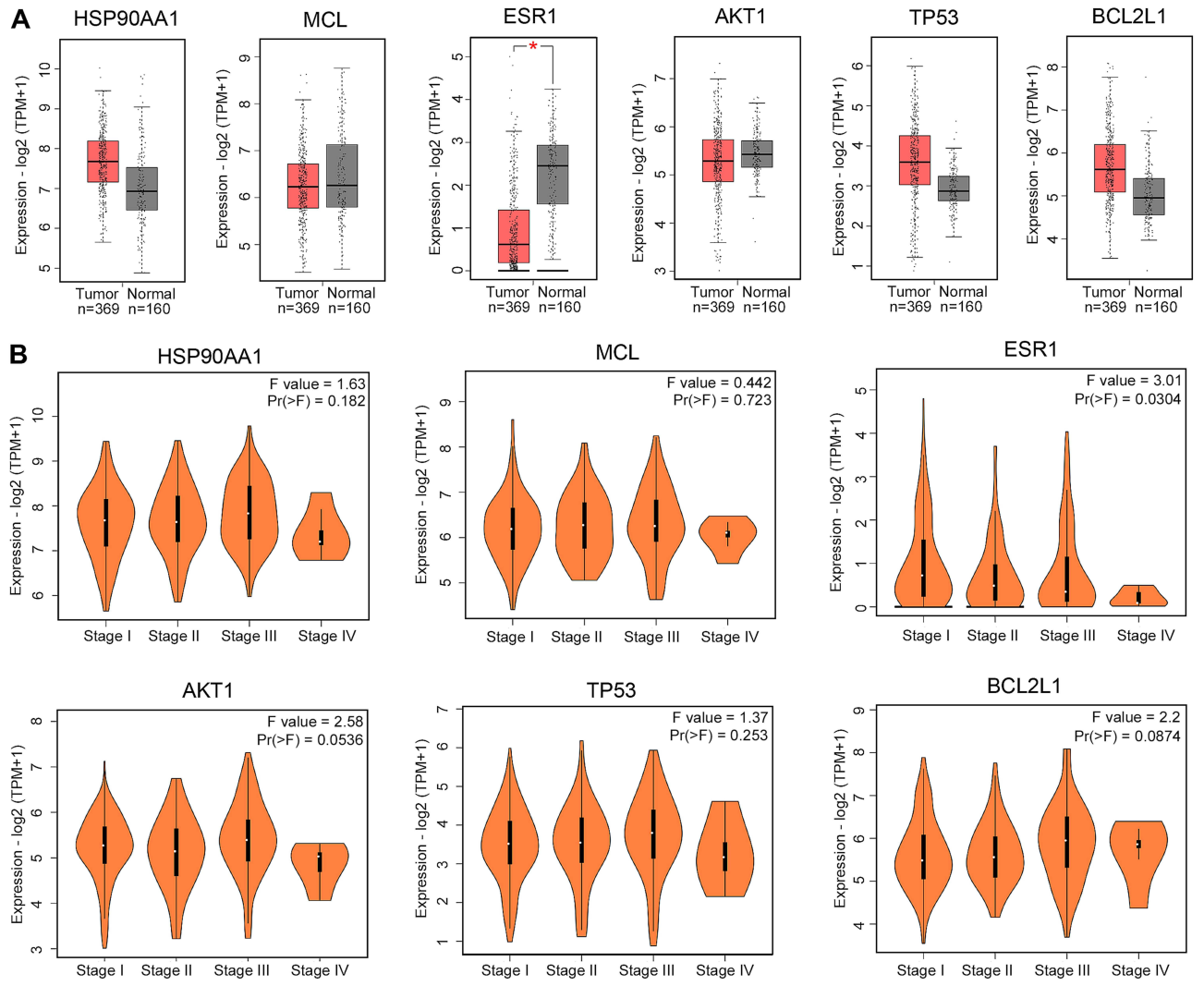

Figure 6 Expression of clinicopathologically relevant genes involved in the risk score formula. (**A**). Expression of *HSP90AA1*, *MCL1*, *ESR1*, *AKT1*, *TP53*, and *BCL2L1* in HCC based on the Cancer Genome Atlas database, *$P < 0.05$. (**B**) Expression of *HSP90AA1*, *MCL1*, *ESR1*, *AKT1*, *TP53*, and *BCL2L1* relevant to the clinical stage of hepatocellular carcinoma.

MDM2, AKT1, ESR1, BCL2L1, MCL1, HSP90AA1, CASP9, and *CCND1*. The abnormal expression of most of these hub genes has been reported to be closely related to HCC progression.

Following bioinformatics analysis, the GO terms related to these 53 genes were explored, and a total of 77 GO terms, including BP, CC, and MF were enriched. We noticed that among the GO annotations, GO:0045429~positive regulation of nitric oxide biosynthetic process was the most significant BP, suggesting that the target genes related to *Codonopsis pilosula* promote the biosynthesis of nitric oxide; GO:0005654~nucleoplasm was the most significant CC, suggesting that the *Codonopsis pilosula*-related target genes are mainly localized in the nucleoplasm and are related to downstream signal transduction; and GO:0019903~protein phosphatase binding was the most significant MF, suggesting that the *Codonopsis pilosula*-related target genes have important protein modification functions. Additionally, the KEGG pathway enrichment results revealed that *Codonopsis pilosula*-related target genes were associated with 72 KEGG signals. The complexity of the KEGG signaling pathway suggests a possible mechanism of multi-network interactions for treating HCC with *Codonopsis pilosula*. We noticed that among these 72 KEGG signals, in addition to tumor and immune-inflammatory signals, some classical signals, such as the hsa04115:p53 signaling pathway, hsa04110:Cell cycle, hsa04915:Estrogen signaling pathway, hsa04012:ErbB signaling pathway, hsa04630:Jak-STAT signaling pathway, hsa04370:VEGF-signaling pathway, and hsa04010:MAPK-signaling pathway, were also enriched.

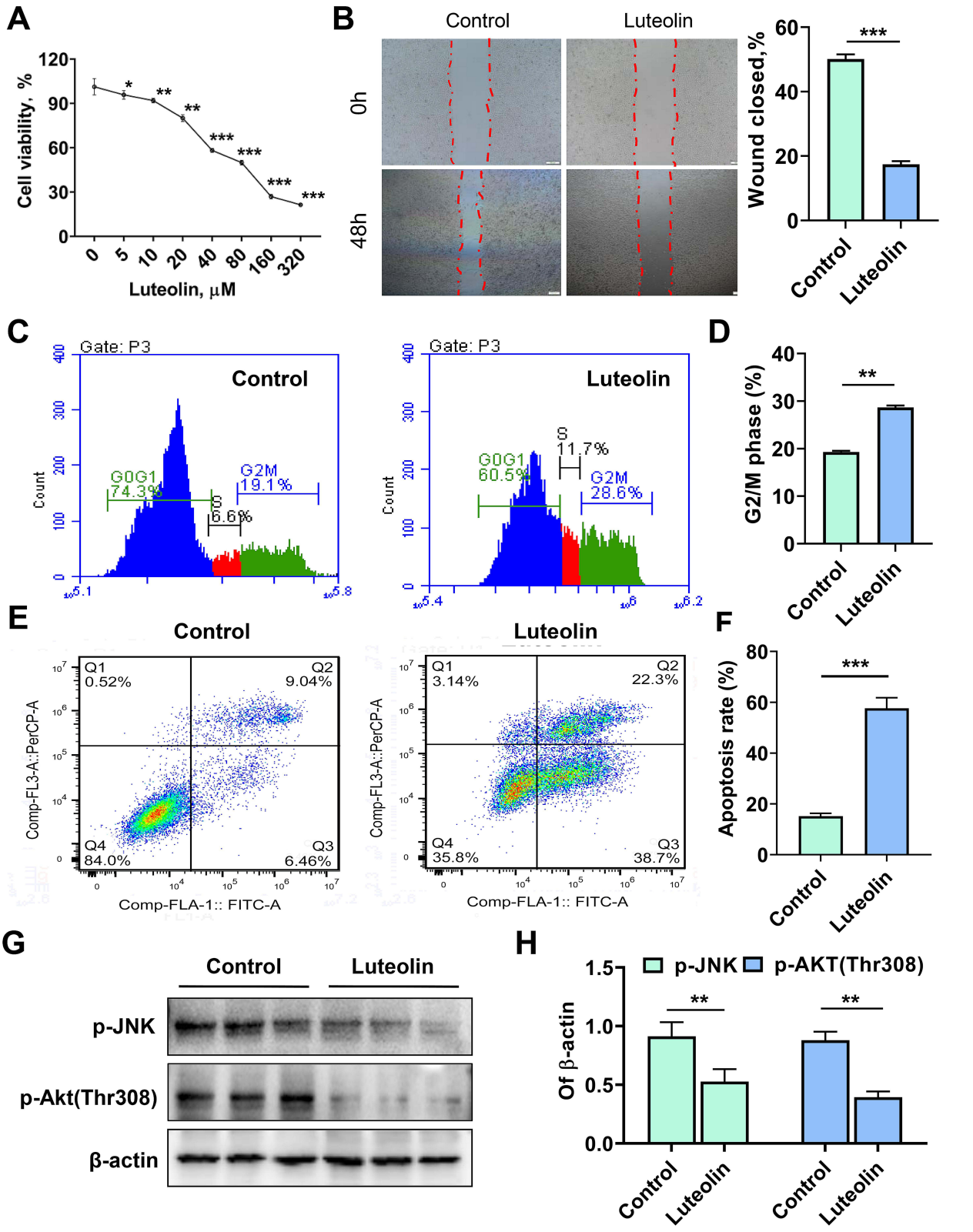

Figure 7 Effects of luteolin-anti hepatocellular carcinoma in vitro. (**A**) The effect of luteolin on the proliferation of HepG2 cells, as assessed by CCK-8 assay. n = 5, post hoc Dunnett's test, $^{*}P < 0.05$, $^{**}P < 0.01$, $^{***}P < 0.001$ vs 0 group. (**B**) Representative images for cell migration. Bars = 200 μm, n = 5, *t*-test, $^{***}P < 0.001$. (**C**) Representative images for FCM detection of the cell cycle distribution. (**D**) Quantitative analysis of cell cycle G2/M phase distribution, n = 3, *t*-test, $^{**}P < 0.01$. (**E**) Representative images for luteolin-induced apoptosis, as assessed by flow cytometry. (**F**) Quantitative results of luteolin-induced apoptosis, n = 3, *t*-test, $^{***}P < 0.001$. (**G**) Representative bands for Western blotting of p-Akt (Thr 308) and p-JNK. (**H**). Quantitative results of p-Akt (Thr308) and p-JNK normalized to GAPDH, n = 6, *t*-test for p-Akt (Thr308), Mann–Whitney test for p-JNK, $^{**}P < 0.01$.

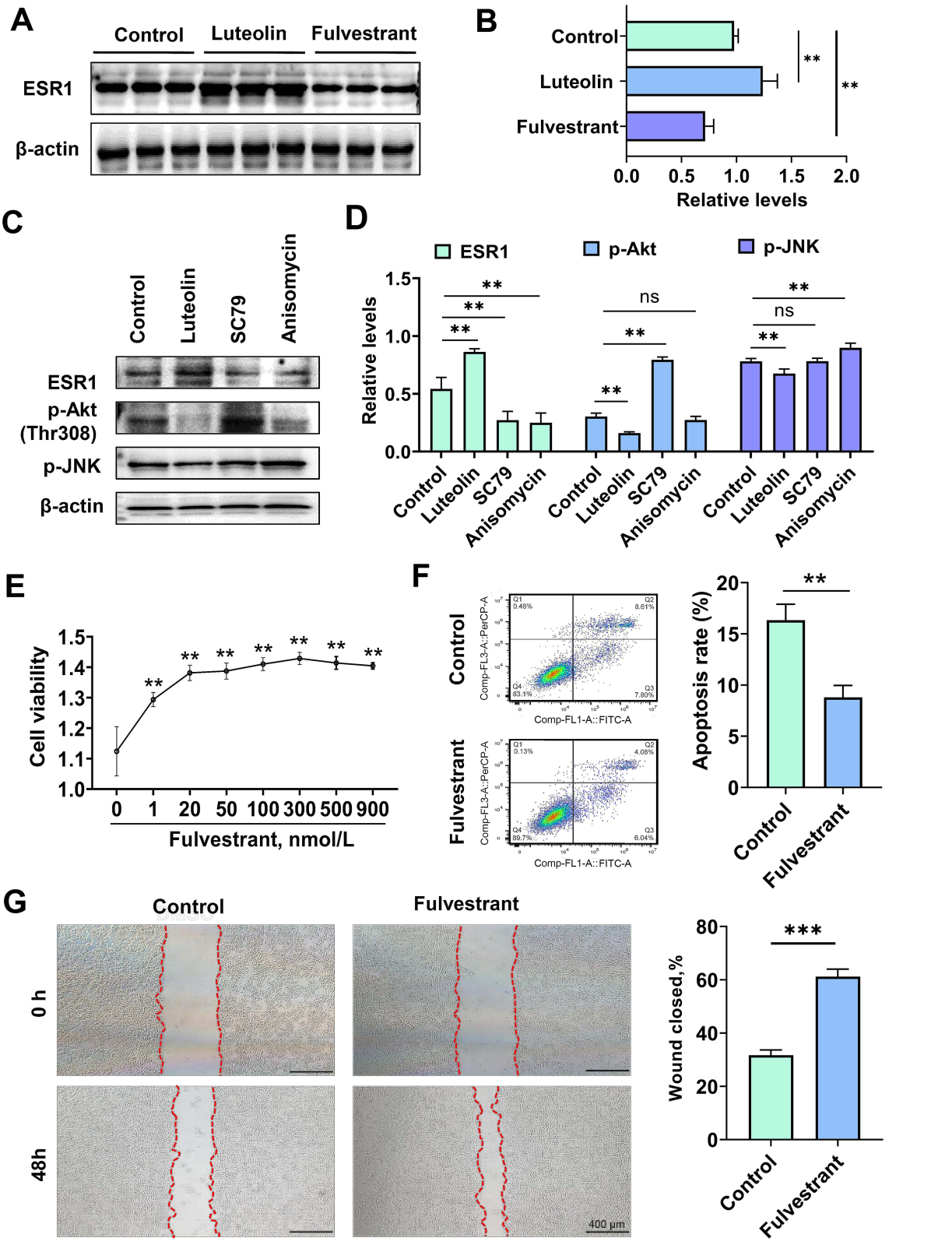

Figure 8 Effects of luteolin on ESR1 expression in hepatocellular carcinoma. (**A**) Representative bands for Western blot analysis of 50 μmol/L luteolin-, 300 nmol/L fulvestrant-induced ESR1 expression. (**B**) Quantitative results of luteolin-, fulvestrant-induced ESR1, n = 6, post hoc Dunnett's test, $^{**}P < 0.01$. (**C**) Representative bands for Western blot analysis of 50 μmol/L luteolin-, 10 μmol/L SC79- and 4 μmol/L anisomycin-induced ESR1, p-Akt (Thr308) and p-JNK. (**D**) Quantitative results of luteolin-, SC79-, and anisomycin-induced ESR1, p-Akt (Thr308) and p-JNK expression, n = 5, post hoc Dunnett's test, $^{**}P < 0.01$. (**E**) The effect of ESR1 inhibitor fulvestrant on the cell viability of HepG2 cells as assessed by CCK-8 assay, n = 5, post hoc Dunnett's test, $^{**}P < 0.01$ vs 0 group. (**F**) ESR1 inhibitor fulvestrant (300 nmol/L) suppressed cell apoptosis, as assessed by flow cytometry, n = 3, *t*-test, $^{**}P < 0.01$. (**G**) ESR1 inhibitor fulvestrant (300 nmol/L) promoted cell migration, n = 5, *t*-test, $^{***}P < 0.001$, Bars = 400 μm.

Abbreviation: ns, no significance.

Based on LASSO Cox regression analysis, we screened six prognostic genes, including *TP53, AKT1, ESR1, BCL2L1, HSP90AA1*, and *CCND1*, from the 10 hub targets for dimensionality reduction to construct the risk model. Among these six selected genes, based on the GEPIA database, *ESR1* and *HSP90AA1* were closely related to the prognosis of HCC. Interestingly, *ESR1* and *HSP90AA1* displayed opposite prognostic signatures in HCC. Interestingly, Jeon et al[28] reported that low expression of *ESR1*-encoded ERα was related to better OS and DFS in patients with HCC. Moreover, Xiao et al[29] proposed that *HSP90AA1* may be a potential biomarker for HCC. Indeed, high expression of HSP90AA1 has been shown to be associated with poor OS in HCC, which is in agreement with the current findings.[30,31] Through establishing a risk prediction model combining the above six factors, we obtained a better prognostic discriminant value. In the TCGA HCC cohort, the high or low risk in our current models indeed appeared a significant prognosis. This signature was further verified by the ROC curves assessing the 1-, 3-, and 5-year AUCs. Thus, our risk predication model has potential clinical application value for the prognosis of *Codonopsis pilosula* for treating HCC but requires further verification using the clinical cohort in the later stage.

We then verified the anti-HCC effects of *Codonopsis pilosula* through the application of luteolin. The results of serial in vitro experiments showed that the application of luteolin significantly inhibited the proliferation and migration of HCC cells, blocked the HCC cell cycle at the G2/M phase, and induced apoptosis of HCC cells. The activation of MAPK-JNK and AKT signaling is critical for cancer cell viability, survival, and migration, and we also found that treatment of HCC cells with luteolin led to attenuated expression of p-JNK and p-Akt (Thr308), implying that luteolin may exert anti-HCC effects by inhibiting MAPK-JNK and AKT signaling.

Finally, to further explore the mechanism of luteolin against HCC, we focused on the ESR1 molecule. Indeed, treatment of HCC cells with luteolin led to upregulation of ESR1 protein levels. We found that luteolin up-regulated ESR1 expression at least through AKT and MAPK-JNK signaling. Inhibition of ESR1 in HepG2 cells enhanced cell viability and migration and attenuated cell apoptosis. Our current study indicated that AKT and MAPK-JNK signaling-meditated ESR1 is involved in the action of luteolin against HCC. Our study also showed that low ESR1 to be an adverse prognostic indicator for OS of HCC. The significance of ESR1 in the prognosis of HCC has drawn considerable attention. Several reports have proposed that a low level of ESR1 was a determinant for HCC tumorigenesis or prognosis.[28,32–34] Our findings supported the conclusion that low ESR1 expression in HCC favors cancer progression and luteolin exerts anti-HCC action partly through mediation of ESR1 expression. Luteolin is a flavonoid found in plants, such as vegetables, fruits, and herbal medicines, which are effective in the treatment of human malignancies.[35] There are also some reports on the application of luteolin monomers in the treatment of HCC, with encouraging findings.[36–40] As an active compound of *Codonopsis pilosula*, the various anti-tumor properties of luteolin highlight the potential anti-HCC effects of *Codonopsis pilosula*.

Recently, Liu et al published a report on the application of network pharmacology to analyze the effects of *Codonopsis pilosula* on HCC.[41] In this report, Liu et al mainly used transcriptomics and network pharmacology to explore the potential molecular mechanisms of *Codonopsis pilosula* in the treatment of HCC.[41] In our investigation, in addition to the application of network pharmacology to explore the mechanism of *Codonopsis pilosula* in the treatment of HCC, we further constructed a risk prediction model of *Codonopsis pilosula* for treating HCC with hub genes. Simultaneously, luteolin, an active ingredient of *Codonopsis pilosula*, was also used to verify its anti-cancer effects. The current study reinforces the effectiveness of *Codonopsis pilosula* as an anti-HCC strategy.

The present study has some shortcomings. First, *Codonopsis pilosula* contains many active ingredients in addition to luteolin, and the anti-HCC function of these active agents must also be established. Second, KEGG results showed that the anti-HCC effect of *Codonopsis pilosula* involves multiple signal pathways. This study only addressed AKT and AMPK-JNK signals. Other signals need to be tested as well. Finally, animal experiments could well supplement the results of this study.

Conclusion

In this study, we combined network pharmacology and bioinformatics technology to explore the effects and mechanism of the active components of *Codonopsis pilosula* against HCC. The results showed that the TCM *Codonopsis pilosula* has multi-component, multi-target, and multi-signal anti-cancer properties. Luteolin, one of the main active ingredients of

Codonopsis pilosula, showed significant ability to inhibit the proliferation, cell cycle, and migration of HCC cells, as well as to induce apoptosis in them. We found that the mechanism by which luteolin acts against HCC may involve AKT- and MAPK-JNK signaling mediated ESR1. These results lay a solid foundation for research into the anti-HCC effects of *Codonopsis pilosula* in the future.

Acknowledgments

We would like to thank LetPub for its linguistic assistance during the preparation of this manuscript.

Author Contributions

All authors made a significant contribution to the work reported, whether that is in the conception, study design, execution, acquisition of data, analysis and interpretation, or in all these areas; took part in drafting, revising, or critically reviewing the article; gave final approval of the version to be published; have agreed on the journal to which the article has been submitted; and agree to be accountable for all aspects of the work.

Funding

This research was funded by grants from the Hainan Province Science and Technology special fund (ZDYF2020143, ZDYF2020132, ZDYF2021SHFZ098, ZDYF2022SHFZ065), the specific research fund of the Innovation Platform for Academicians of Hainan Province (YSPTZX202208) and the Hainan Province Clinical Medical Center (QWYH202175).

Disclosure

The authors have no conflicts of interest related to this work.

References

1. Bray F, Ferlay J, Soerjomataram I, Siegel RL, Torre LA, Jemal A. Global cancer statistics 2018: GLOBOCAN estimates of incidence and mortality worldwide for 36 cancers in 185 countries. *CA Cancer J Clin*. 2018;68(6):394–424. doi:10.3322/caac.21492
2. Sung H, Ferlay J, Siegel RL, et al. Global cancer statistics 2020: GLOBOCAN estimates of incidence and mortality worldwide for 36 cancers in 185 countries. *CA Cancer J Clin*. 2021;71(3):209–249. doi:10.3322/caac.21660
3. Xia C, Dong X, Li H, et al. Cancer statistics in China and United States, 2022: profiles, trends, and determinants. *Chin Med J*. 2022;135(5):584–590. doi:10.1097/CM9.0000000000002108
4. Cao M, Li H, Sun D, Chen W. Cancer burden of major cancers in China: a need for sustainable actions. *Cancer Commun*. 2020;40(5):205–210. doi:10.1002/cac2.12025
5. Villanueva A. Hepatocellular Carcinoma. *N Engl J Med*. 2019;380(15):1450–1462. doi:10.1056/NEJMra1713263
6. Pinero F, Dirchwolf M, Pessoa MG. Biomarkers in hepatocellular carcinoma: diagnosis, prognosis and treatment response assessment. *Cells*. 2020;9(6):1370. doi:10.3390/cells9061370
7. Qiu Z, Li H, Zhang Z, et al. A pharmacogenomic landscape in human liver cancers. *Cancer Cell*. 2019;36(2):179–193 e11. doi:10.1016/j.ccell.2019.07.001
8. Liu C, Yang S, Wang K, et al. Alkaloids from Traditional Chinese Medicine against hepatocellular carcinoma. *Biomed Pharmacother*. 2019;120:109543. doi:10.1016/j.biopha.2019.109543
9. Dong S, Zhuang X, Yangyang L, et al. Efficacy and safety of acupuncture combined with Chinese herbal medicine in the treatment of primary liver cancer: a protocol for systematic review and meta-analysis. *Medicine*. 2021;100(40):e27497. doi:10.1097/MD.0000000000027497
10. Tsai F-J, Liu X, Chen C-J, et al. Chinese herbal medicine therapy and the risk of overall mortality for patients with liver cancer who underwent surgical resection in Taiwan. *Complement Ther Med*. 2019;47:102213. doi:10.1016/j.ctim.2019.102213
11. Liao Y-H, Lin C-C, Lai H-C, Chiang J-H, Lin J-G, Li T-C. Adjunctive traditional Chinese medicine therapy improves survival of liver cancer patients. *Liver Int*. 2015;35(12):2595–2602. doi:10.1111/liv.12847
12. Tang S, Liu W, Zhao Q, et al. Combination of polysaccharides from Astragalus membranaceus and Codonopsis pilosula ameliorated mice colitis and underlying mechanisms. *J Ethnopharmacol*. 2021;264:113280. doi:10.1016/j.jep.2020.113280
13. Hu Y, Sun J, Wang T, et al. Compound Danshen Dripping Pill inhibits high altitude-induced hypoxic damage by suppressing oxidative stress and inflammatory responses. *Pharm Biol*. 2021;59(1):1585–1593. doi:10.1080/13880209.2021.1998139
14. Zou Y-F, Zhang -Y-Y, Paulsen BS, et al. New pectic polysaccharides from Codonopsis pilosula and Codonopsis tangshen: structural characterization and cellular antioxidant activities. *J Sci Food Agric*. 2021;101(14):6043–6052. doi:10.1002/jsfa.11261
15. Zhang P, Hu L, Bai R, et al. Structural characterization of a pectic polysaccharide from Codonopsis pilosula and its immunomodulatory activities in vivo and in vitro. *Int J Biol Macromol*. 2017;104(Pt A):1359–1369. doi:10.1016/j.ijbiomac.2017.06.023
16. Bai R-B, Zhang Y-J, Fan J-M, et al. Immune-enhancement effects of oligosaccharides from Codonopsis pilosula on cyclophosphamide induced immunosuppression in mice. *Food Funct*. 2020;11(4):3306–3315. doi:10.1039/c9fo02969a
17. Huo J, Qin F, Cai X, et al. Chinese medicine formula "Weikang Keli" induces autophagic cell death on human gastric cancer cell line SGC-7901. *Phytomedicine*. 2013;20(2):159–165. doi:10.1016/j.phymed.2012.10.001

18. Liu H, Amakye WK, Ren J. Codonopsis pilosula polysaccharide in synergy with dacarbazine inhibits mouse melanoma by repolarizing M2-like tumor-associated macrophages into M1-like tumor-associated macrophages. *Biomed Pharmacother*. 2021;142:112016. doi:10.1016/j.biopha.2021.112016
19. Liu Y, Zou X, Sun G, Bao Y. Codonopsis lanceolata polysaccharide CLPS inhibits melanoma metastasis via regulating integrin signaling. *Int J Biol Macromol*. 2017;103:435–440. doi:10.1016/j.ijbiomac.2017.05.093
20. Gong Y-B, Fu S-J, Wei Z-R, Liu J-G, Rehman G. Predictive study of the active ingredients and potential targets of Codonopsis pilosula for the treatment of osteosarcoma via network pharmacology. *Evid Based Complement Alternat Med*. 2021;2021:1480925. doi:10.1155/2021/1480925
21. Jiang N, Li H, Sun Y, et al. Network pharmacology and pharmacological evaluation reveals the mechanism of the sanguisorba officinalis in suppressing hepatocellular carcinoma. *Front Pharmacol*. 2021;12:618522. doi:10.3389/fphar.2021.618522
22. Zhang S, Mo Z, Zhang S, Li X. A network pharmacology approach to reveal the underlying mechanisms of Artemisia annua on the treatment of hepatocellular carcinoma. *Evid Based Complement Alternat Med*. 2021;2021:8947304. doi:10.1155/2021/8947304
23. Yang A-L, Wu Q, Hu Z-D, et al. A network pharmacology approach to investigate the anticancer mechanism of cinobufagin against hepatocellular carcinoma via downregulation of EGFR-CDK2 signaling. *Toxicol Appl Pharmacol*. 2021;431:115739. doi:10.1016/j.taap.2021.115739
24. Ru J, Li P, Wang J, et al. TCMSP: a database of systems pharmacology for drug discovery from herbal medicines. *J Cheminform*. 2014;6(1):13. doi:10.1186/1758-2946-6-13
25. Ding R, Qu Y, Wu CH, Vijay-Shanker K. Automatic gene annotation using GO terms from cellular component domain. *BMC Med Inform Decis Mak*. 2018;18(Suppl S5):119. doi:10.1186/s12911-018-0694-7
26. Deng Y, Ye X, Chen Y, et al. Chemical characteristics of Platycodon grandiflorum and its mechanism in lung cancer treatment. *Front Pharmacol*. 2021;11:609825. doi:10.3389/fphar.2020.609825
27. Dong Y, Hao L, Fang K, et al. A network pharmacology perspective for deciphering potential mechanisms of action of Solanum nigrum L. in bladder cancer. *BMC Complement Med Ther*. 2021;21(1):45. doi:10.1186/s12906-021-03215-3
28. Jeon Y, Yoo JE, Rhee H, et al. YAP inactivation in estrogen receptor alpha-positive hepatocellular carcinoma with less aggressive behavior. *Exp Mol Med*. 2021;53(6):1055–1067. doi:10.1038/s12276-021-00639-2
29. Xiao H, Wang B, Xiong HX, et al. A novel prognostic index of hepatocellular carcinoma based on immunogenomic landscape analysis. *J Cell Physiol*. 2021;236(4):2572–2591. doi:10.1002/jcp.30015
30. Chen YQ, Zheng L, Zhou J, et al. Evaluation of plasma LC3B(+)extracellular vesicles as a potential novel diagnostic marker for hepatocellular carcinoma. *Int Immunopharmacol*. 2022;108:108760. doi:10.1016/j.intimp.2022.108760
31. Chen W, Li G, Peng J, Dai W, Su Q, He Y. Transcriptomic analysis reveals that heat shock protein 90 alpha is a potential diagnostic and prognostic biomarker for cancer. *Eur J Cancer Prev*. 2020;29(4):357–364. doi:10.1097/CEJ.0000000000000549
32. Yu J, Ma S, Tian S, et al. Systematic construction and validation of a prognostic model for hepatocellular carcinoma based on immune-related genes. *Front Cell Dev Biol*. 2021;9:700553. doi:10.3389/fcell.2021.700553
33. Hu X, Pan H, Zhou S, et al. HS1BP3, transcriptionally regulated by ESR1, promotes hepatocellular carcinoma progression. *Biochem Biophys Res Commun*. 2022;623:111–119. doi:10.1016/j.bbrc.2022.07.047
34. Wu H, Yao S, Zhang S, et al. Elevated expression of Erbin destabilizes ERalpha protein and promotes tumorigenesis in hepatocellular carcinoma. *J Hepatol*. 2017;66(6):1193–1204. doi:10.1016/j.jhep.2017.01.030
35. Imran M, Rauf A, Abu-Izneid T, et al. Luteolin, a flavonoid, as an anticancer agent: a review. *Biomed Pharmacother*. 2019;112:108612. doi:10.1016/j.biopha.2019.108612
36. Im E, Yeo C, Lee EO. Luteolin induces caspase-dependent apoptosis via inhibiting the AKT/osteopontin pathway in human hepatocellular carcinoma SK-Hep-1 cells. *Life Sci*. 2018;209:259–266. doi:10.1016/j.lfs.2018.08.025
37. Elsayed MMA, Okda TM, Atwa GMK, Omran GA, Abd Elbaky AE, Ramadan AEH. Design and optimization of orally administered luteolin nanoethosomes to enhance its anti-tumor activity against hepatocellular carcinoma. *Pharmaceutics*. 2021;13(5):648. doi:10.3390/pharmaceutics13050648
38. Cai S, Bai Y, Wang H, et al. Knockdown of THOC1 reduces the proliferation of hepatocellular carcinoma and increases the sensitivity to cisplatin. *J Exp Clin Cancer Res*. 2020;39(1):135. doi:10.1186/s13046-020-01634-7
39. Lee HJ, Wang CJ, Kuo HC, Chou FP, Jean LF, Tseng TH. Induction apoptosis of luteolin in human hepatoma HepG2 cells involving mitochondria translocation of Bax/Bak and activation of JNK. *Toxicol Appl Pharmacol*. 2005;203(2):124–131. doi:10.1016/j.taap.2004.08.004
40. Yee SB, Choi HJ, Chung SW, et al. Growth inhibition of luteolin on HepG2 cells is induced via p53 and Fas/Fas-ligand besides the TGF-beta pathway. *Int J Oncol*. 2015;47(2):747–754. doi:10.3892/ijo.2015.3053
41. Liu Z, Sun Y, Zhen H, Nie C. Network pharmacology integrated with transcriptomics deciphered the potential mechanism of codonopsis pilosula against hepatocellular carcinoma. *Evid Based Complement Alternat Med*. 2022;2022:1340194. doi:10.1155/2022/1340194